



Published in final edited form as:

Int J Biochem Cell Biol. 2014 December ; 57: 7–19. doi:10.1016/j.biocel.2014.09.018.

Activation of the Nlrp3 inflammasome by mitochondrial reactive oxygen species: A novel mechanism of albumin-induced tubulointerstitial inflammation

Dan Liu^a, Min Xu^a, Li-Hong Ding^a, Lin-Li Lv^a, Hong Liu^a, Kun-Ling Ma^a, Ai-Hua Zhang^b, Steven D. Crowley^c, and Bi-Cheng Liu^{a,*}

^aInstitute of Nephrology, Zhong Da Hospital, Southeast University School of Medicine, Nanjing, Jiangsu, China

^bInstitute of Pediatrics, Department of Nephrology, Nanjing Children's Hospital, Nanjing Medical University, Nanjing, Jiangsu, China

^cDivision of Nephrology, Department of Medicine, Duke University and Durham VA Medical Centers, Durham, NC, United States

Abstract

Albuminuria is not only an important marker of chronic kidney disease but also a crucial contributor to tubulointerstitial inflammation (TIF). In this study, we determined whether activation of the Nlrp3 inflammasome is involved in albuminuria induced-TIF and the underlying mechanisms of inflammasome activation by mitochondrial reactive oxygen species (mROS). We established an albumin-overload induced rat nephropathy model characterised by albuminuria, renal infiltration of inflammatory cells, tubular dilation and atrophy. The renal expression levels of the Nlrp3 inflammasome, IL-1 β and IL-18 were significantly increased in this animal model. In vitro, albumin time- and dose-dependently increased the expression levels of the Nlrp3 inflammasome, IL-1 β and IL-18. Moreover, the silencing of the Nlrp3 gene or the use of the caspase-1 inhibitor Z-VAD-fmk significantly attenuated the albumin-induced increase in IL-1 β and IL-18 expression in HK2 cells. In addition, mROS generation was elevated by albumin stimulation, whereas the ROS scavenger N-acetyl-L-cysteine (NAC) inhibited Nlrp3 expression and the release of IL-1 β and IL-18. In kidney biopsy specimens obtained from patients with IgA nephropathy, Nlrp3 expression was localised to the proximal tubular epithelial cells, and this result is closely correlated with the extent of proteinuria and TIF. In summary, this study demonstrates that albuminuria may serve as an endogenous danger-associated molecular pattern (DAMP) that stimulates TIF via the mROS-mediated activation of the cytoplasmic Nlrp3 inflammasome.

Keywords

Nlrp3 inflammasome; Albuminuria; Mitochondrial reactive oxygen species; Proximal tubular epithelial cell; Tubulointerstitial inflammation

© 2014 Elsevier Ltd. All rights reserved.

*Corresponding author. Present address: Institute of Nephrology, Zhong Da Hospital, Southeast University School of Medicine, Nanjing 210009, China., Tel.: +86 2583272090; fax: +86 2583272090., liubc64@163.com (B.-C. Liu).

1. Introduction

Tubulointerstitial inflammation plays a central role in the loss of renal function in chronic renal disease, but the exact mechanism remains largely unknown (Lee and Kalluri, 2010). A number of studies have demonstrated that albuminuria is not only a well-recognised hallmark of kidney disease but also a pathogenic factor involved in the development of proteinuric nephropathy, which is characterised by alterations in proximal tubular epithelial cell (PTEC) death and inflammatory cytokine production (Abbate et al., 2006; Baines and Brunskill, 2011; Eddy and Giachelli, 1995; Li et al., 2010). Albuminuria stimulates proximal tubular cells to synthesise chemokines (MCP-1 and RANTES) that recruit monocytes and T cells and contributes to the release of cytokines that attract neutrophils and fibrosis-promoting molecules (e.g., endothelin, angiotensin II, and TGF- α) through phospholipase C, MAPK, or NF- κ B signal activation (Drumm et al., 2002; Gomez-Garre et al., 2001; Gorriz and Martinez-Castelao, 2012; Han et al., 2005; Liu et al., 2009; Takase et al., 2008; Wang et al., 1999). These studies raised a concern about the pathogenic role of proteinuria in the progression of chronic renal disease. However, the exact molecular mechanisms that regulate inflammation by albuminuria have not been fully elucidated.

More recent studies have focused on innate immune-sensing receptors and their role in inflammation and disease processes. The Nlrp3 inflammasome is a cytoplasmic multiprotein that contains the Nod-like receptor and ASC adaptor (Lorenz et al., 2014) and triggers the activation of caspase-1, IL-1 β and IL-18 to engage innate immune defences and execute inflammatory responses (Latz et al., 2013; Schroder and Tschopp, 2010; Shi et al., 2012). Previous studies have confirmed that the inflammasome is activated by a variety of stimuli, including pathogens associated with virtually every type of pathogen-associated molecular pattern (PAMP). It is also triggered by several danger signals, including pore-forming toxins from bacteria, extracellular ATP (Mariathasan et al., 2006), ROS (Martinon et al., 2009; Zhou et al., 2010), monosodium urate crystals (Martinon et al., 2006), nucleic acids (Muruve et al., 2008), extracellular matrix components, including hyaluronan (Yamasaki et al., 2009), biglycans (Babelova et al., 2009), and environmental microparticles, such as asbestos and silica (Dostert et al., 2008; Martinon, 2012). The activation of the Nlrp3 inflammasome requires a two-step signal. Initially, the transcription and translation of immature pro-IL-1 β (pro-IL-18) mRNA is induced via NF- κ B activation by a primary signal, which may be derived from TLR, TNFR or IL-1R signalling. A secondary signal then activates the inflammasome and cleaves mature IL-1 β /IL-18 released by inflammasome stimuli (Gross et al., 2011; Lorenz et al., 2014).

A strong association between dysregulated inflammasome activity and certain human inflammatory diseases suggests the importance of this pathway in innate immune responses, such as gouty arthritis (Martinon et al., 2006), type 2 diabetes mellitus, atherosclerosis, and inflammatory bowel disease (Strowig et al., 2012). Previous studies have demonstrated that IL-18 and caspase-1, which are two key markers of Nlrp3 inflammasome activation, are expressed in the renal tubular epithelium of patients with chronic kidney disease, suggesting that the Nlrp3 inflammasome may play an important role in regulating inflammation in kidney diseases (Gauer et al., 2007; Lonnemann et al., 2003). However, the role of albuminuria in the activation of the tubular Nlrp3 inflammasome and its subsequent

contribution to tubulointerstitial inflammation remains speculative. The purpose of this study was therefore to investigate whether albuminuria directly induces mROS generation to activate the Nlrp3 inflammasome pathway in tubular cells during the genesis of tubulointerstitial inflammation.

2. Materials and methods

2.1. Animal model

Protein-overload nephropathy (Eddy, 1989) was induced via intraperitoneal injection of bovine serum albumin (BSA) in male Wistar rats one week after right nephrectomy (initial weight 120–130 g, Academy of Military Medical Science, Animal Experiment Centre). The rats were fed standard rat chow ad libitum, given free access to water and randomly divided into two groups. In the albumin-overload group (AO, $n = 10$), the rats were administered a daily intraperitoneal injection of BSA (5.0 g/kg/d, fatty acid-free, low endotoxin, Roche). The rats in the control group ($n = 8$) received an intraperitoneal injection of an equivalent volume of saline at pH 7.4. BSA was dissolved in normal saline at a concentration of 33% (pH 7.4). The BSA injection was sustained for nine weeks. At the end of week 10, the animals were anaesthetised with chloral hydrate and sacrificed. The animal care protocols and experimental protocol used in this study were approved by the Ethics Review Committees for Animal Experimentation of Southeast University.

2.2. Urine and blood measurements

The body weight was measured weekly. Samples were collected every 24 h from rats housed in metabolic cages for 0, 2, 5, 7, 9 and 10 weeks with access to drinking water only. The urinary protein and albumin excretion were measured using the Coomassie Blue method (Jiancheng, Nanjing) or an ELISA kit according to the manufacturer's instructions. The urinary N-acetyl- β -D-glycosaminidase (NAG) levels were measured using an ELISA kit (Jiancheng, Nanjing). Blood samples were collected on weeks 0, 2, 5, 7, 9 and 10 (at death) from the inner canthus or heart after sacrifice in the 10th week to assess the changes in biochemical parameters (Hitachi, Tokyo, Japan).

2.3. Renal histological preparation and assessment

The left kidneys were collected after perfusion with 50 ml of ice-cold normal saline. A portion of coronal tissue was fixed with 10% buffered formalin and then embedded in paraffin for staining with haematoxylin-eosin (HE), periodic acid-Schiff reagent (PAS), and immunohistochemistry. To assess the pathological scoring for tubular injury, the PAS-stained slides (3 μ m-thick sections) were reviewed by two independent renal pathologists in a blinded manner. A tubular injury scoring system adapted from Vilaysane et al. (2010) was used. The percentage of cortical tubular necrosis was assigned a score as follows: 0 = normal, 1 = <20%, 2 = 20–40%, 3 = 40–60%, 4 = 60–80%, and 5 = >80%. The levels of tubulointerstitial inflammation in 20 randomly selected non-overlapping fields from the kidney of each rat or IgAN patient were scored at 400 \times magnification with periodic acid-Schiff staining. The scoring of interstitial inflammatory cell infiltration in each specimen was as follows: 0 = normal, 1 = <25% of the interstitium was affected, 2 = 25–50% of the interstitium was affected, and 3 = >50% of the interstitium was affected (Yu et al., 2010).

2.4. Immunohistochemistry staining

For analysis and localising the expression of the endocytic receptors, the components of the renal tubular Nlrp3 inflammasome were examined. Briefly, paraffin-embedded sections from the kidney cortex were incubated with primary antibodies to Nlrp3, caspase-1, ASC, IL-18 (Santa Cruz Biotechnology, USA) and IL-1 β (Cell Signalling Technology, USA), and the sections from renal biopsies of patients with IgA nephropathy were incubated with primary antibodies to Nlrp3 and IL-18. The sections were then analysed using an appropriate immunohistochemical kit processing (Maxim, China) according to the manufacturer's instructions. An immunohistochemistry semiquantitative analysis was conducted using the Image Pro Plus image analysis system.

2.5. Electron microscopy analysis

For transmission electron microscopy (TEM) observations of ultrastructural changes in proximal tubular epithelial cells, the kidneys or collected HK-2 cell clusters were immersed in a fixative containing 2.5% glutaraldehyde and 4% paraformaldehyde in 0.1 M phosphate buffer. After fixation and dehydration with ethanol, the samples were embedded in Durcupan resin for ultra-thin sectioning and TEM examination in the VCU electron microscopy core facility.

2.6. Tubular epithelial cell isolation and mitochondrial extraction

The renal capsule was removed, and the cortex was dissected from the medulla. The cortex was then finely minced to 1–2 mm³, washed with PBS, spun three times at 800 \times g, placed in collagenase A (Sigma–Aldrich, St. Louis, MO), and incubated at 37 °C for 30 min with frequent shaking. After incubation, the digested mixture was differentially sieved through descending pore sizes (80, 100, and 200 mesh) and washed three times with fresh media. The sieved contents were then centrifuged, pelleted, and layered over 25 ml of 45% Percoll (Sigma–Aldrich, USA). After spinning the Percoll mixture at 17,200 \times g for 30 min, four distinct bands were apparent, as previously described (McLaren et al., 1995). The cells from the third band were collected and washed three times with HBSS. The mitochondria from the tubular epithelial cells were then extracted using a mitochondrial isolation kit (Abcam, USA) according to the manufacturer's protocol. The obtained mitochondria were frozen at –80 °C with a protease inhibitor cocktail for western blot or prepared for assaying the mitochondrial membrane potential (MMP, Ψ).

2.7. JC-1 examination

In vitro, living tubular epithelial cells (HK-2) were digested by trypsin in six-well plates, and the mitochondria from the tubular epithelial cell were isolated in vivo. In both mitochondrial preparations, the MMP values were quantified using a JC-1 kit (KeyGEN BioTECH, China) to measure the uptake of the fluorescent dye JC-1 by the mitochondria and then subjected to a fluorescence microplate reader test, fluorescence microscopy observations, or a flow cytometry assay.

2.8. Cell culture and siRNA treatment

A tubular epithelial cell line (HK-2) was purchased from the China Centre for Type Culture Collection (CCTCC) and cultured in specialised tubular epithelial cell growth media (DMEM–Ham's-F-12 [GIBCO, USA]; insulin [5 µg/ml]; transfer-rin [5 µg/ml]; hydrocortisone [0.4 µg/ml; Sigma–Aldrich]; and penicillin G/streptomycin [100 U/ml penicillin G and 100 µg/ml streptomycin; Hyclone, USA]; and 10% foetal bovine serum [GIBCO, Uruguay]). The transfection reagents and siRNA for Nlrp3 were obtained from Invitrogen (RNAiMax reagent and Stealth RNAi™). The non-targeting scramble-sequence siRNA (Stealth RNAi™) was used as a negative control. Cultured HK-2 cells were transfected according to the manufacturer's protocol (Invitrogen, USA).

2.9. Supernatant ELISA detection

The IL-1β and IL-18 contents in cell-free supernatants were measured using a Valukine™ ELISA kit (R&D Systems, USA), according to the manufacturer's instructions.

2.10. Flow cytometric analyses

The mitochondrial mass was measured based on fluorescence levels through staining with Mitotracker Green and Mitotracker Red CMXRos at 100 nM for 30 min at 37 °C. The mitochondria-associated ROS levels were measured by staining the cells with 5 µM MitoSOX for 20 min at 37 °C. The HK-2 cell mitochondria membrane potential was measured using the JC-1 assay kit from Invitrogen according to the manufacturer's instructions. The intracellular ROS generation can be investigated using 2',7'-dichlorofluorescein-diacetate (DCFH-DA, Sigma–Aldrich). The cells were then washed with PBS solution and re-suspended in cold PBS solution containing 1% FBS for FACS analysis.

2.11. Quantitative real-time RT-PCR analyses

The total RNA from HK-2 cells or tubular epithelial cells isolated from the kidney cortex was extracted using the RNAiso plus reagent, and cDNA was then synthesised using a reverse transcription (RT) system kit (Takara, Japan) according to the manufacturer's instructions. Real-time RT-PCR was performed using an ABI PRISM 7300 real-time PCR System (Applied Biosystems, USA). This assay was used to determine the degree of Nlrp3 inflammasome activation through measuring the levels of Nlrp3, ASC, IL-1β, and IL-18 gene expression. GAPDH served as a control for the reaction efficiency of the target genes. The results were analysed using the comparative cycle threshold (Ct) method.

2.12. Western blotting assays

Western blot analysis using whole-cell lysates and cell culture supernatants was performed as described previously (Hornung et al., 2008; Liu et al., 2009). The cell culture supernatants (400 µl) were lysed, precipitated by the addition of an equal volume of methanol and 0.25 volumes of chloroform, vortexed and centrifuged for 10 min at 20,000 × g. The upper phase was discarded, and 500 µl of methanol was added to the interphase. This mixture was centrifuged for 10 min at 20,000 × g, and the protein pellet was dried at 55 °C, resuspended in Laemmli buffer and boiled for 5 min at 99 °C. The protein lysates from the HK-2 cells and kidney cortex extracts were lysed using a total protein extraction kit (KeyGEN, China)

according to the manufacturer's instructions, separated by SDS-PAGE, and then transferred onto PVDF membranes (Millipore) blocked with 5% milk proteins. The membranes were then incubated overnight at 4 °C with the following primary antibodies: anti-Nlrp3, IL-1 β , IL-18, ASC, caspase-1, MCP-1, IL-6 (Santa Cruz Biotechnology, USA), and IL-1 β (Cell Signaling technology, USA). The blots were washed and incubated with secondary horseradish peroxidase-conjugated antibodies as appropriate, and the signals were then detected using an ECL advanced system (GE Healthcare, UK).

2.13. Confocal microscopy

HK-2 cells were plated on confocal dishes for 2 d and then subjected to albumin stimulation. At the end of the experiments, the cells were stained with Mitotracker Red CMXRos (100 nM). After washing two times with PBST, the cells were fixed with 4% PFA in PBS for 15 min at 37 °C and then washed three times with PBST. After permeabilisation with Triton X-100 and blocking with 10% BSA in PBS, the cells were incubated with primary antibodies (in 5% BSA) overnight at 4 °C. After washing with PBST, the cells were incubated with fluorescent secondary antibodies (Invitrogen) in 5% BSA-PBS for 60 min and rinsed with PBST. The cell nuclei were stained with DAPI (Invitrogen, USA). After BSA stimulation, living HK-2 cells were stained with MitoSOX (5 μ M) for 20 min, and the cells were then washed three times with HBSS. After Hoechst 33,342 staining for detection of the cell nucleus, the stained cells were immediately visualised under a confocal microscope. The confocal microscopy analyses were performed using an Olympus FV 1000 Viewer.

2.14. Statistical analysis

All of the data are expressed as the means \pm SD and analysed by one-way ANOVA using the SPSS 20.0 statistical software. The non-parametric data were analysed using the Mann-Whitney *U* test. *P* values less than 0.05 were considered statistically significant. The correlation analyses were performed using the Spearman rank-order correlation. *P* < 0.05 was considered statistically significant.

3. Results

3.1. Biochemical and pathological changes in experimental rats

To explore the role of albuminuria-induced renal epithelial damage and tubulointerstitial inflammation, we treated Wistar rats with daily injections of 5 g/kg bovine serum albumin (BSA) or normal saline for nine weeks. It was found that rats with albumin overload (AO) presented significantly increased protein excretion and urine albumin levels starting on week 2 (Fig. 1A and B). In addition, N-acetyl- β -D-glycosaminidase (NAG), an accepted marker of tubular injury, was also overtly increased in the AO group starting on week 2 (Fig. 1C). In contrast, no measurable differences in any of these parameters were found in the control group (Fig. 1A–D). PTEC demonstrated atrophy, flattening and deletion from the basement membrane, and these effects were accompanied by marked protein cast formation and tubular dilatation in AO rats, as determined by PAS staining (Fig. 1E). The tubular injury score found for the AO group was markedly elevated relative to the controls (Fig. 1F). Furthermore, we detected a significant correlation between the interstitial inflammatory cell

infiltration scores and proteinuria in albumin-overload rats (Fig. 1G). These findings indicate that albuminuria induces tubular injury and interstitial inflammation.

3.2. Nlrp3 inflammasome activation and inflammatory cytokine production in the albumin-overload animal model

As an indication of Nlrp3 activation, we detected elevated levels of cleaved IL-1 β and IL-18 in the lysates from the kidneys of AO rats but not in those from the controls (Fig. 2A and C). Moreover, we measured the Nlrp3, ASC and caspase-1 expression levels in the kidney lysates and found that they were significantly increased in the AO group (Fig. 2A and B). To clarify whether the exaggerated cytokine production accrued from the tubular compartment and contributed to the TIF, we isolated the tubular epithelial cells from the renal cortex. Consistent with the protein expression levels in the whole kidney cortex, the mRNA levels of the Nlrp3 inflammasome and associated cytokines were markedly increased in tubular cells (Fig. 2D). In addition, immunohistochemistry staining analyses showed that Nlrp3, ASC, cleaved caspase-1, revealed IL-18 and IL-1 β were overexpressed in the PTEC of AO rats (Fig. 2E and F).

3.3. Nlrp3 expression and Nlrp3 inflammasome activation due to albumin stimulation in HK-2 cells

To confirm that albuminuria stimulates Nlrp3 expression and Nlrp3 inflammasome activation, we performed further in vitro studies in which we exposed HK-2 cells to different doses of albumin over a range of time periods. Based on the western blot analysis of the cell lysates, the levels of Nlrp3 and ASC proteins were upregulated by albumin treatment in a time (6, 12, 24, and 48 h of incubation)- and dose (5, 10, 20, and 40 mg/ml of BSA)-dependent manner with peaks at 24 h and 20 mg/ml, respectively (Fig. 3A–D). Moreover, we found that cleaved caspase-1, IL-1 β and IL-18 emerged in the culture supernatant over the same time frame (Fig. 3A–D). The secreted IL-18 in the culture supernatants was significantly increased in a time-dependent and dose-dependent manner in the supernatant after BSA stimulation, as measured by ELISA (Fig. 3E and F), but IL-1 β was undetectable (data not shown). In addition, Nlrp3 and ASC were distributed in the cytoplasm of resting cells, however, Nlrp3 protein expression and ASC speck formation were co-localized into the perinuclear space after incubation with albumin, as observed by confocal microscopy (Fig. 3G). Collectively, albumin overload triggered Nlrp3 expression and Nlrp3 inflammasome activation in HK-2 cells, leading to the production of cleaved IL-1 β and IL-18.

3.4. Albumin stimulation in HK-2 cells drives the production of mature IL-18 and IL-1 β by activating the Nlrp3 inflammasome

Because mature IL-18 and IL-1 β are markers of Nlrp3 inflammasome activation, we wondered whether the overexpression of these cytokines in albumin-treated HK-2 cells was induced via Nlrp3 inflammasome activation. Therefore, HK-2 cells were transfected with siRNA for Nlrp3 24 h prior to albumin overload (20 mg/ml), yielding 81.2% Nlrp3 knockdown (Fig. 4A and B). The inhibition of Nlrp3 by siRNA almost completely prevented the inflammasome activation and significantly blocked the albumin-triggered IL-18 and IL-1 β secretion (Fig. 4C–E). In addition, the specific peptide inhibitor of caspase-1 Z-VAD-

fmk abolished the release of IL-18 and IL-1 β in response to treatment with 20 mg/ml albumin (Fig. 4F). These data suggest that albumin triggers IL-18 and IL-1 β production via an Nlrp3-caspase-1-dependent pathway in HK-2 cells.

3.5. Albuminuria triggers mitochondrial dysfunction and mROS generation

To determine the mechanism through which albuminuria triggers Nlrp3 inflammasome activation in the renal epithelia, we examined the ultrastructure of kidney tissue by TEM and found that the boundaries between epithelial cells of the tubular wall were blurred with a thickening of the tubular basement membrane in the experimental rats (Fig. 5A). Some tubular cells were flattened or had numerous vacuoles in the cytoplasm. The mitochondria displayed balloon-like changes with oedema, brightened matrix, and reduced numbers of cristae. In contrast, the renal tubular cells from the saline-treated control rats displayed normal ultrastructural features. To further demonstrate mitochondrial injury in the AO rats, we measured the mitochondrial transmembrane potential (MMP) levels in mitochondria extracted from isolated renal tubular cells using the fluorescent dye JC-1 to avoid contamination from other renal parenchymal cells (Fig. 5B and C). MMP staining was significantly reduced ten weeks following albumin injection compared with saline. These data suggest that albumin induces mitochondrial dysfunction and may thus promote tubular cell stress and interstitial inflammation.

We also used TEM to demonstrate the ultrastructure alterations in albumin-treated HK-2 cells in vitro. Compared with the controls (Fig. 6A), these cells developed numerous vacuoles in the cytoplasm, abnormal swollen mitochondria with a brightened matrix and destroyed cristae, and abundant autophagic vesicles. Moreover, the total ROS production was measured by FACS using DCFH-DA, which has been widely used as a marker for oxidative stress (Fig. 6B). The JC-1 staining revealed MMP degradation in living HK-2 cells after albumin treatment (Fig. 6C). MMP is essential for the maintenance of normal mitochondrial function, and the MMP level in HK-2 cells was therefore determined using mitochondria-specific labels to distinguish the total mitochondria (Mitotracker Green FM) and the MMP-deficient mitochondria (Mitotracker Red CMXRos) (Fig. 6D). The intracellular production or accumulation of mitochondrial-generating ROS after BSA stimulation was measured with the intracellular detection probe MitoSOX Red, a special mitochondrial indicator, in living HK-2 cells (Fig. 6E and F). These measurements indicate that albumin induces ROS release and accumulation in living HK-2 cells.

3.6. Albumin-induced Nlrp3 inflammasome activation is prevented by a ROS scavenger in HK-2 cells

Because ROS have been proposed to mediate Nlrp3 activation, we speculated that albumin overload causes mitochondrial dysfunction, leading to ROS release and accumulation with consequent Nlrp3 inflammasome activation. To test this possibility, NAC, which functions as a scavenger of ROS, was added to HK-2 cells during albumin treatment. As expected, NAC reduced the mROS (MitoSOX) release and alleviated the MMP diminution (Mitotracker Red CMXRos and Mitotracker Green) induced by albumin exposure (Fig. 6D–F). The caspase-1, IL-18, and IL-1 β release in the culture supernatants were effectively inhibited by incubation with NAC prior to albumin exposure (Fig. 7A–C). To determine

whether the degree of Nlrp3 inflammasome activation was correlated with the mROS level, we examined the localisation of Nlrp3 in HK-2 cell lines through confocal microscopy (Fig. 7D). Under normal conditions, most of the Nlrp3 protein was scattered throughout the cytoplasm in granular structures, and the mitochondria assumed a long, filamentous morphology. There was almost no overlap between the Nlrp3 mitochondrial stains. However, following albumin stimulation, the mitochondria were fragmented and co-localised with Nlrp3 abutting the nuclear envelope. The addition of NAC prior to BSA exposure prevented Nlrp3 upregulation and co-localisation with fissured mitochondria. These results suggest that albumin-related Nlrp3 activation depends on the release of mROS from dysfunctional mitochondria.

3.7. The kidney expression of Nlrp3 inflammasome in patients with IgA nephropathy correlates with the extent of proteinuria

IgA nephropathy (IgAN) is the most common glomerulonephritis worldwide and is characterised by the deposition of IgA antibody in the glomerulus and proteinuria. To confirm whether the tubular injury in IgAN is associated with albumin-induced-Nlrp3 inflammasome activation, we quantified the protein levels of Nlrp3 and IL-18, which are markers of inflammasome activation, in kidney biopsy samples of IgAN patients through immunohistochemistry. Minimal expression of Nlrp3 and IL-18 was noted in the mild proteinuria group (proteinuria < 1 g/24 h). However, with higher levels of proteinuria, the expression levels of Nlrp3 and IL-18 were significantly increased (Fig. 8A), such that there were significant positive correlations between the extent of proteinuria and the Nlrp3 or IL-18 expression levels (Fig. 8B). Furthermore, the Nlrp3 and IL-18 expression levels were also correlated with inflammatory cell infiltration into the renal interstitium (Fig. 8C).

4. Discussion

The presence of persistent amounts of albumin in urine is a sign of kidney damage and a predictor of disease progression. The potential mechanism underlying how albumin impacts the progression to CKD remains unknown. Many studies have demonstrated a positive correlation between the degree of albuminuria and disease progression and confirmed the tubular toxic nature of albuminuria (Abbate et al., 2006; Baines and Brunskill, 2011; Eddy, 1989; Eddy and Giachelli, 1995; Thomas et al., 1999). To understand the contribution and mechanism of albuminuria results in tubulointerstitial damage, we constructed a albuminuria-toxicity model, which is a non-immunological model of proteinuria and tubulointerstitial injury as a result of direct albumin inoculation (Chang et al., 2012; Eddy, 1989; Eddy and Giachelli, 1995). A key observation of this study is that the Nlrp3 inflammasome and downstream cytokines were upregulated in albumin-overloaded rats and biopsy specimens from IgAN patients with severe proteinuria.

The Nlrp3 inflammasome is a cytosolic multiprotein platform that senses environmental or cellular danger signals to promote inflammation (Schroder and Tschopp, 2010). A variety of stimuli have been demonstrated to activate the Nlrp3 inflammasome, such as endogenous DAMPs and crystals (Martinon, 2012; Menu and Vince, 2011). Recent evidence describes a role for CaOx crystals and uromodulin in triggering IL-1 β -dependent innate immunity via the Nlrp3/ASC/caspase-1 axis in intrarenal mononuclear phagocytes and in directly

In conclusion, we demonstrated that albuminuria induces TIF through mROS-dependent Nlrp3 inflammasome activation. Our characterisation of the Nlrp3 inflammasome in experimental albumin-overload kidney disease sheds new light on the proteinuria toxic effects involved in interstitial inflammation and also supports a role for Nlrp3 in human proteinuric nephropathies (Fig. 9). Our findings emphasise the importance of clinical anti-proteinuric strategies and highlight Nlrp3 inflammasome inhibition as a promising method for arresting the progression of proteinuric kidney disease. Finally, these may provide theoretical evidence on the potential of anakinra, an interleukin-1 (IL-1) receptor antagonist, for proteinuric kidney disease therapies.

Acknowledgments

This study was supported by grants from the National Natural Scientific Foundation (No. 81130010), the Clinic Research Center of Jiangsu Province (No. BL2014080). No part of this manuscript has been published elsewhere or has been submitted to another journal. All of the co-authors have read and agree with the contents of this manuscript, and there are no financial interests to report.

Abbreviations

TIF	tubulointerstitial inflammation
NLR	nucleotide-binding domain leucine-rich repeat-containing (protein/family)
ASC	apoptosis-associated speck-like protein containing a CARD
siRNA	small interfering RNA
NAC	N-acetyl-L-cysteine
Z-VAD-fmk	N-benzyloxycarbonyl-Val-Ala-Asp-fluoromethyl ketone

References

- Abbate M, Zoja C, Remuzzi G. How does proteinuria cause progressive renal damage? *J Am Soc Nephrol.* 2006; 17:2974–84. [PubMed: 17035611]
- Babelova A, Moreth K, Tsalastra-Greul W, Zeng-Brouwers J, Eickelberg O, Young MF, et al. Biglycan, a danger signal that activates the NLRP3 inflammasome via toll-like and P2X receptors. *J Biol Chem.* 2009; 284:24035–48. [PubMed: 19605353]
- Baines RJ, Brunskill NJ. Tubular toxicity of proteinuria. *Nat Rev Nephrol.* 2011; 7:177–80. [PubMed: 21151210]
- Cassel SL, Eisenbarth SC, Iyer SS, Sadler JJ, Colegio OR, Tephly LA, et al. The Nalp3 inflammasome is essential for the development of silicosis. *Proc Natl Acad Sci U S A.* 2008; 105:9035–40. [PubMed: 18577586]
- Chang AM, Ohse T, Krofft RD, Wu JS, Eddy AA, Pippin JW, et al. Albumin-induced apoptosis of glomerular parietal epithelial cells is modulated by extracellular signal-regulated kinase 1/2. *Nephrol Dial Transplant.* 2012; 27:1330–43. [PubMed: 21896500]
- Chen K, Zhang J, Zhang W, Zhang J, Yang J, Li K, et al. ATP-P2X4 signaling mediates NLRP3 inflammasome activation: a novel pathway of diabetic nephropathy. *Int J Biochem Cell Biol.* 2013; 45:932–43. [PubMed: 23434541]
- Cruz CM, Rinna A, Forman HJ, Ventura AL, Persechini PM, Ojcius DM. ATP activates a reactive oxygen species-dependent oxidative stress response and secretion of proinflammatory cytokines in macrophages. *J Biol Chem.* 2007; 282:2871–9. [PubMed: 17132626]

- Darisipudi MN, Thomasova D, Mulay SR, Brech D, Noessner E, Liapis H, et al. Uromodulin triggers IL-1beta-dependent innate immunity via the NLRP3 inflammasome. *J Am Soc Nephrol*. 2012; 23:1783–9. [PubMed: 22997256]
- Dostert C, Petrilli V, Van Bruggen R, Steele C, Mossman BT, Tschopp J. Innate immune activation through Nalp3 inflammasome sensing of asbestos and silica. *Science*. 2008; 320:674–7. [PubMed: 18403674]
- Drumm K, Bauer B, Freudinger R, Gekle M. Albumin induces NF-kappaB expression in human proximal tubule-derived cells (IHKE-1). *Cell Physiol Biochem*. 2002; 12:187–96. [PubMed: 12297724]
- Eddy AA. Interstitial nephritis induced by protein-overload proteinuria. *Am J Pathol*. 1989; 135:719–33. [PubMed: 2801886]
- Eddy AA, Giachelli CM. Renal expression of genes that promote interstitial inflammation and fibrosis in rats with protein-overload proteinuria. *Kidney Int*. 1995; 47:1546–57. [PubMed: 7643523]
- Eder C. Mechanisms of interleukin-1beta release. *Immunobiology*. 2009; 214:543–53. [PubMed: 19250700]
- Fang L, Xie D, Wu X, Cao H, Su W, Yang J. Involvement of endoplasmic reticulum stress in albuminuria induced inflammasome activation in renal proximal tubular cells. *PLOS ONE*. 2013; 8:e72344. [PubMed: 23977286]
- Gauer S, Sichler O, Obermuller N, Holzmann Y, Kiss E, Sobkowiak E, et al. IL-18 is expressed in the intercalated cell of human kidney. *Kidney Int*. 2007; 72:1081–7. [PubMed: 17687255]
- Gomez-Garre D, Largo R, Tejera N, Fortes J, Manzarbeitia F, Egido J. Activation of NF-kappaB in tubular epithelial cells of rats with intense proteinuria: role of angiotensin II and endothelin-1. *Hypertension*. 2001; 37:1171–8. [PubMed: 11304520]
- Gorritz JL, Martinez-Castelao A. Proteinuria: detection and role in native renal disease progression. *Transplant Rev (Orlando)*. 2012; 26:3–13. [PubMed: 22137726]
- Gross O, Thomas CJ, Guarda G, Tschopp J. The inflammasome: an integrated view. *Immunol Rev*. 2011; 243:136–51. [PubMed: 21884173]
- Han HJ, Oh YJ, Lee YJ. Effect of albumin on 14C-alpha-methyl-D-glucopyranoside uptake in primary cultured renal proximal tubule cells: involvement of PLC, MAPK, and NF-kappaB. *J Cell Physiol*. 2005; 202:246–54. [PubMed: 15389529]
- Hornung V, Bauernfeind F, Halle A, Samstad EO, Kono H, Rock KL, et al. Silica crystals and aluminum salts activate the NALP3 inflammasome through phagosomal destabilization. *Nat Immunol*. 2008; 9:847–56. [PubMed: 18604214]
- Latz E, Xiao TS, Stutz A. Activation and regulation of the inflammasomes. *Nat Rev Immunol*. 2013; 13:397–411. [PubMed: 23702978]
- Lee SB, Kalluri R. Mechanistic connection between inflammation and fibrosis. *Kidney Int Suppl*. 2010:S22–6. [PubMed: 21116313]
- Li X, Pabla N, Wei Q, Dong G, Messing RO, Wang CY, et al. PKC-delta promotes renal tubular cell apoptosis associated with proteinuria. *J Am Soc Nephrol*. 2010; 21:1115–24. [PubMed: 20395372]
- Lichtnekert J, Kulkarni OP, Mulay SR, Rupanagudi KV, Ryu M, Allam R, et al. Anti-GBM glomerulonephritis involves IL-1 but is independent of NLRP3/ASC inflammasome-mediated activation of caspase-1. *PLoS ONE*. 2011; 6:e26778. [PubMed: 22046355]
- Liu BC, Gao J, Li Q, Xu LM. Albumin caused the increasing production of angiotensin II due to the dysregulation of ACE/ACE2 expression in HK2 cells. *Clin Chim Acta*. 2009; 403:23–30. [PubMed: 19141296]
- Lonnemann G, Novick D, Rubinstein M, Dinarello CA. Interleukin-18, interleukin-18 binding protein and impaired production of interferon-gamma in chronic renal failure. *Clin Nephrol*. 2003; 60:327–34. [PubMed: 14640238]
- Lorenz G, Darisipudi MN, Anders HJ. Canonical and non-canonical effects of the NLRP3 inflammasome in kidney inflammation and fibrosis. *Nephrol Dial Transplant*. 2014; 29:41–8. [PubMed: 24026244]
- Mariathasan S, Weiss DS, Newton K, McBride J, O'Rourke K, Roose-Girma M, et al. Cryopyrin activates the inflammasome in response to toxins and ATP. *Nature*. 2006; 440:228–32. [PubMed: 16407890]

- Martinon F. Signaling by ROS drives inflammasome activation. *Eur J Immunol.* 2010; 40:616–9. [PubMed: 20201014]
- Martinon F. Dangerous liaisons: mitochondrial DNA meets the NLRP3 inflammasome. *Immunity.* 2012; 36:313–5. [PubMed: 22444626]
- Martinon F, Mayor A, Tschopp J. The inflammasomes: guardians of the body. *Annu Rev Immunol.* 2009; 27:229–65. [PubMed: 19302040]
- Martinon F, Petrilli V, Mayor A, Tardier A, Tschopp J. Gout-associated uric acid crystals activate the NALP3 inflammasome. *Nature.* 2006; 440:237–41. [PubMed: 16407889]
- McLaren J, Whiting P, Simpson J, Hawks worth G. Isolation and characterisation of human proximal tubular cells derived from kidney cortical segments. *Human Exp Toxicology.* 1995; 14:916–22.
- Menu P, Vince JE. The NLRP3 inflammasome in health and disease: the good, the bad and the ugly. *Clin Exp Immunol.* 2011; 166:1–15. [PubMed: 21762124]
- Mulay SR, Kulkarni OP, Rupanagudi KV, Migliorini A, Darisipudi MN, Vilaysane A, et al. Calcium oxalate crystals induce renal inflammation by NLRP3-mediated IL-1beta secretion. *J Clin Invest.* 2013; 123:236–46. [PubMed: 23221343]
- Muruve DA, Petrilli V, Zaiss AK, White LR, Clark SA, Ross PJ, et al. The inflammasome recognizes cytosolic microbial and host DNA and triggers an innate immune response. *Nature.* 2008; 452:103–7. [PubMed: 18288107]
- Schroder K, Tschopp J. The inflammasomes. *Cell.* 2010; 140:821–32. [PubMed: 20303873]
- Shi CS, Shenderov K, Huang NN, Kabat J, Abu-Asab M, Fitzgerald KA, et al. Activation of autophagy by inflammatory signals limits IL-1beta production by targeting ubiquitinated inflammasomes for destruction. *Nat Immunol.* 2012; 13:255–63. [PubMed: 22286270]
- Strowig T, Henao-Mejia J, Elinav E, Flavell R. Inflammasomes in health and disease. *Nature.* 2012; 481:278–86. [PubMed: 22258606]
- Takase O, Minto AW, Puri TS, Cunningham PN, Jacob A, Hayashi M, et al. Inhibition of NF-kappaB-dependent Bcl-xL expression by clusterin promotes albumin-induced tubular cell apoptosis. *Kidney Int.* 2008; 73:567–77. [PubMed: 18075502]
- Thomas ME, Brunskill NJ, Harris KP, Bailey E, Pringle JH, Furness PN, et al. Protein-uria induces tubular cell turnover: a potential mechanism for tubular atrophy. *Kidney Int.* 1999; 55:890–8. [PubMed: 10027925]
- Tschopp J. Mitochondria Sovereign of inflammation? *Eur J Immunol.* 2011; 41:1196–202. [PubMed: 21469137]
- Vilaysane A, Chun J, Seamone ME, Wang W, Chin R, Hirota S, et al. The NLRP3 inflammasome promotes renal inflammation and contributes to CKD. *J Am Soc Nephrol.* 2010; 21:1732–44. [PubMed: 20688930]
- Wang Y, Rangan GK, Tay YC, Wang Y, Harris DC. Induction of monocyte chemoattractant protein-1 by albumin is mediated by nuclear factor kappaB in proximal tubule cells. *J Am Soc Nephrol.* 1999; 10:1204–13. [PubMed: 10361858]
- Wen H, Miao EA, Ting JP. Mechanisms of NOD-like receptor-associated inflammasome activation. *Immunity.* 2013; 39:432–41. [PubMed: 24054327]
- Yamasaki K, Muto J, Taylor KR, Cogen AL, Audish D, Bertin J, et al. NLRP3/cryopyrin is necessary for interleukin-1beta (IL-1beta) release in response to hyaluronan, an endogenous trigger of inflammation in response to injury. *J Biol Chem.* 2009; 284:12762–71. [PubMed: 19258328]
- Yu F, Wu LH, Tan Y, Li LH, Wang CL, Wang WK, et al. Tubulointerstitial lesions of patients with lupus nephritis classified by the 2003 International Society of Nephrology and Renal Pathology Society system. *Kidney Int.* 2010; 77:820–9. [PubMed: 20182417]
- Zhou R, Tardier A, Thorens B, Choi I, Tschopp J. Thioredoxin-interacting protein links oxidative stress to inflammasome activation. *Nat Immunol.* 2010; 11:136–40. [PubMed: 20023662]
- Zhou R, Yazdi AS, Menu P, Tschopp J. A role for mitochondria in NLRP3 inflammasome activation. *Nature.* 2011; 469:221–5. [PubMed: 21124315]

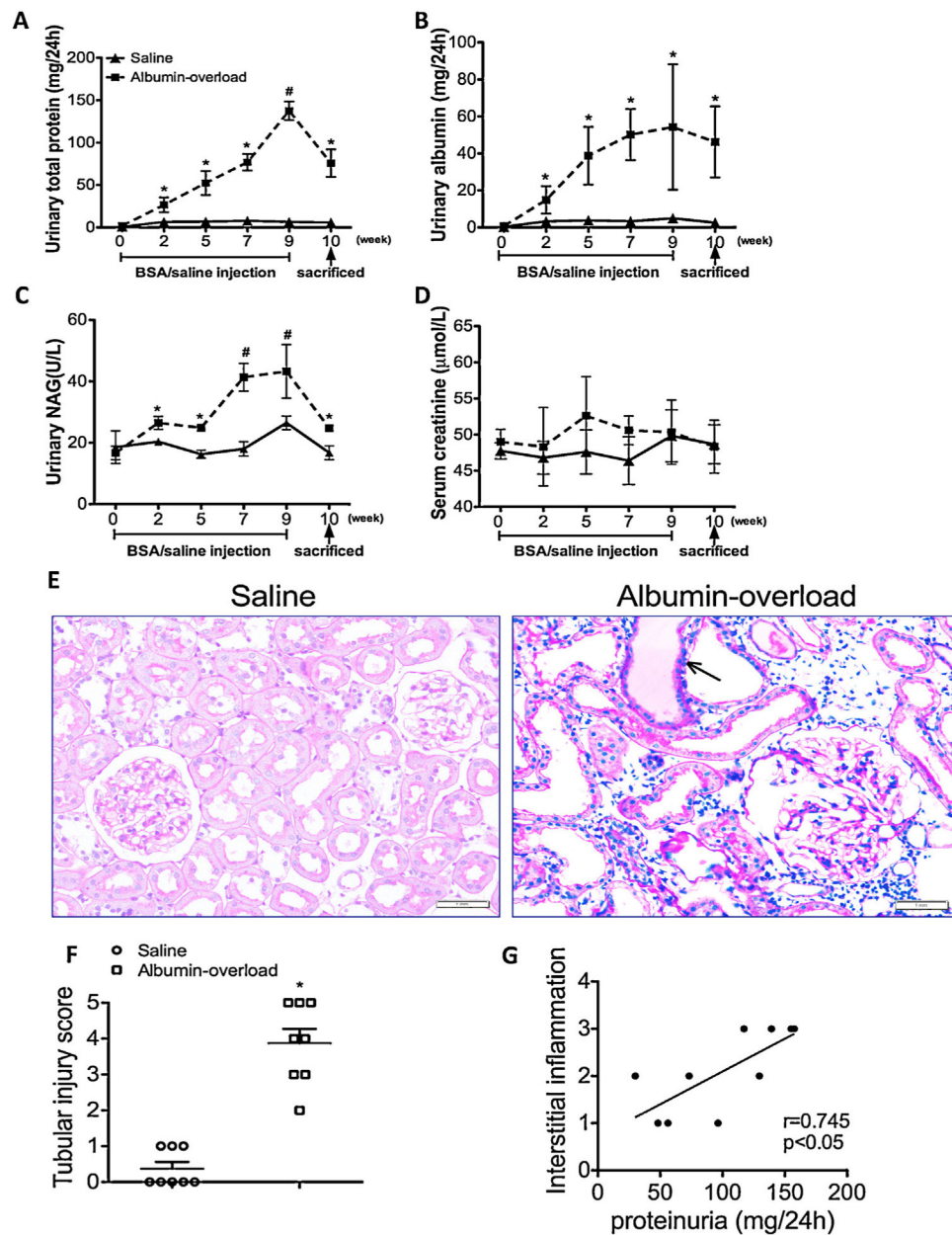


Fig. 1. Proteinuria, tubular injury and biochemical examination of the experimental rats. (A and B) Time course of the appearance of proteinuria and albuminuria. (C) ELISA for NAG in the urine of albumin-overloaded rats compared with those that received the saline injection. (D) Time course of the creatinine level in serum samples of animal models. The data are the means \pm SD ($n = 6$, * $P < 0.05$ and # $P < 0.001$ vs. the saline-treated group). (E) PAS staining of the kidney. The arrow indicates the protein cast in the tubular lumen. (F) Tubular injury scores obtained for the saline-treated group and the albumin-overloaded group. The data are the mean scores ($n = 8$, * $P < 0.05$ for the comparison of the albumin-overloaded group vs. the saline-treated group). (G) Correlation of interstitial inflammatory cell infiltration after

albumin injection and the degree of proteinuria. The data were compared using the Spearman correlation coefficient.

Author Manuscript

Author Manuscript

Author Manuscript

Author Manuscript

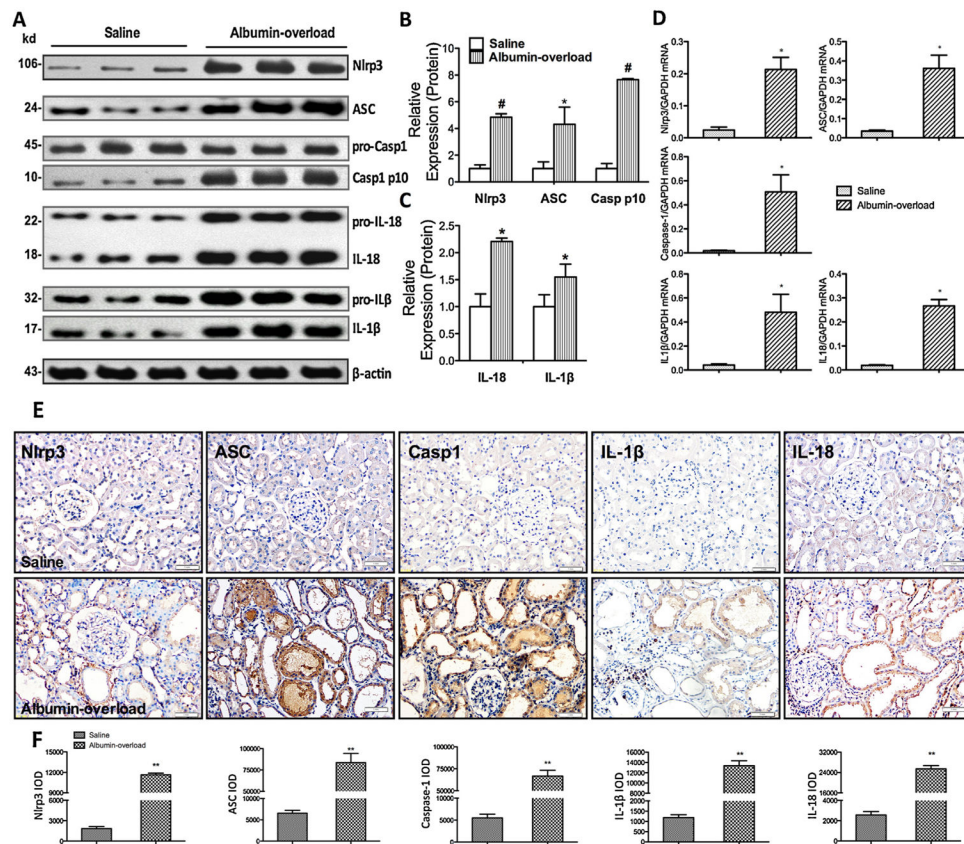


Fig. 2. Nlrp3 inflammasome activation and pro-inflammatory cytokine release in an albumin-overloaded animal model. (A) Nlrp3, ASC, caspase-1, IL-18, and IL-1 β expression in rats after albumin overload or saline injection. Western blotting of kidney tissue lysates from Wistar rats at 10 weeks. The saline-treated group was used as a control. (B and C) Quantification of the expression levels of these proteins in the saline-treated and albumin-overloaded rats normalised to β -actin. The data are the means \pm s.d. ($n = 8$, $*P < 0.05$ and $^{\#}P < 0.001$ vs. the saline-treated group). (D) Nlrp3, ASC, caspase-1, IL-18, and IL-1 β mRNA expression in tubular epithelial cells isolated from kidney tissue at 10 weeks, as measured by quantitative RT-PCR. The data are shown as the means \pm s.d. ($n = 6$, $*P < 0.05$ and $^{\#}P < 0.001$ vs. the saline-treated group). (E) Immunohistochemistry analysis of Nlrp3, ASC, caspase-1, IL-1 β , and IL-18 expression and localisation in the kidney tissue. (F) Semiquantitative immunohistochemistry staining analysis according to the IOD using the Image-Pro plus software. The data are the means \pm SD from five visual fields for one section ($n = 5$, $**P < 0.001$ vs. the saline-treated group).

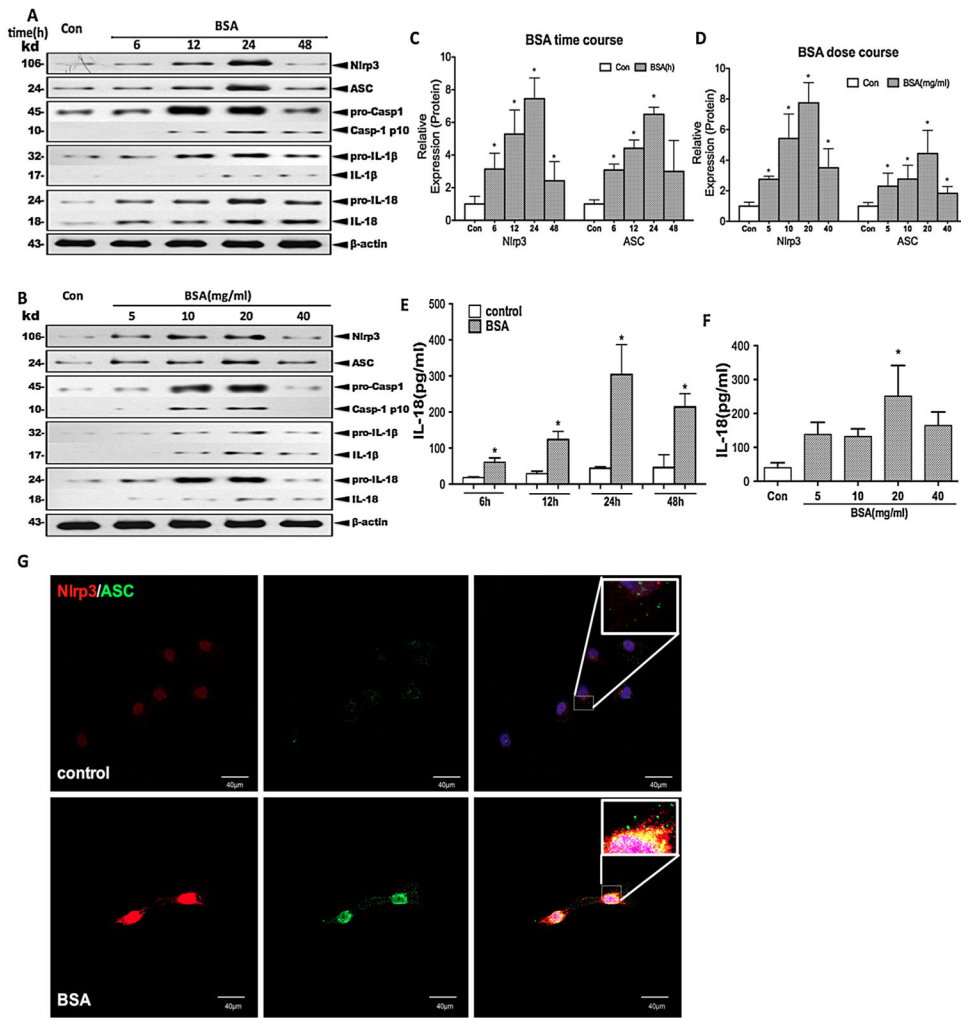


Fig. 3. Albumin overload triggers Nlrp3 inflammasome activation and pro-inflammatory cytokine secretion in cultured HK-2 cells. (A and B) The levels of Nlrp3, ASC, pro-caspase-1, pro-IL-1 β , and pro-IL-18 (cell lysates) and processed caspase-1, IL-1 β , and IL-18 (supernatant) in HK-2 cells after incubation with different doses (5, 10, 20, and 40 mg/ml) of BSA for different times (6, 12, 24, and 48 h) were examined by western blotting. (C and D) Quantification of the protein expression levels. The data are presented as the means \pm SD from three independent experiments. $*P < 0.05$ vs. the control group. (E and F) ELISA detection of IL-18 expression in the supernatant after stimulation with different doses of BSA for different times. (G) The Nlrp3 (red) and ASC (green) protein distribution after BSA (20 mg/ml) treatment for 24 h was localised by confocal microscopy.

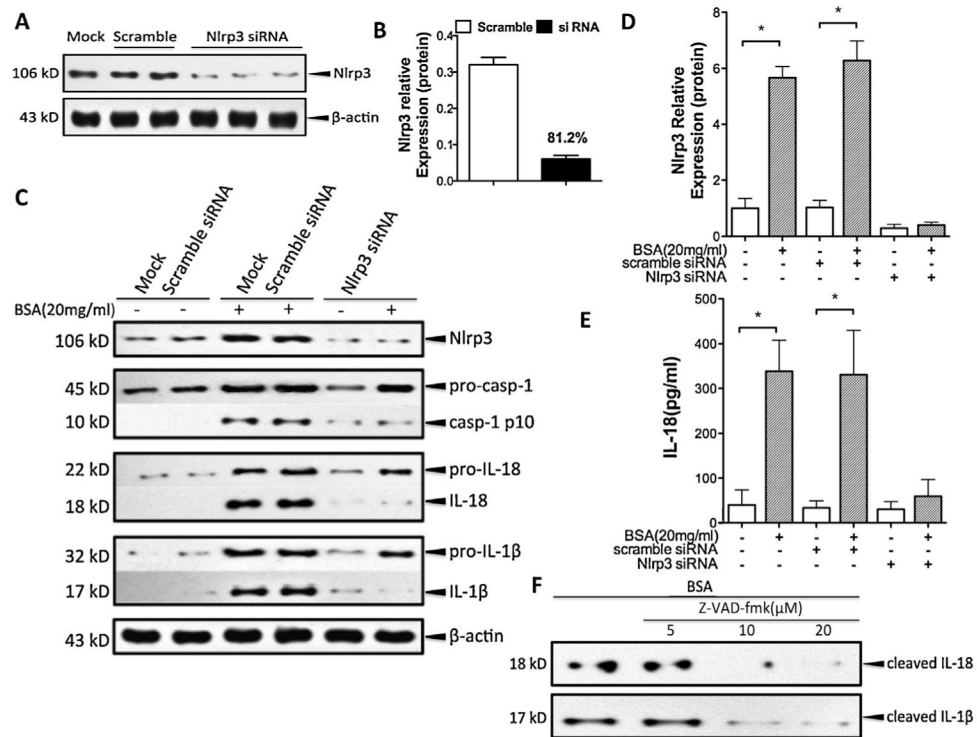


Fig. 4. Albuminuria-induced IL-18 and IL-1 β secretion was dependent on the Nlrp3-caspase-1 pathway in HK-2 cells. (A) HK-2 cells were transfected with small interfering RNA for Nlrp3, and the Nlrp3 protein expression was then analysed by western blotting. The non-targeting scramble-sequence siRNA (scramble) was used as the negative control. (B) Quantitative analysis of the Nlrp3 siRNA transfection knockdown efficiency through western blotting. (C) The levels of Nlrp3, ASC, pro-caspase-1, pro-IL-1 β , and pro-IL-18 (cell lysates) and processed caspase-1, IL-1 β , and IL-18 (supernatant) in HK-2 cells transfected with Nlrp3 siRNA after exposure to albumin (20 mg/ml) for 24 h were detected by western blotting and compared with the control (mock and scramble). (D) Quantification of Nlrp3 expression normalised to that of β -actin. (E) The secreted IL-18 in the cell supernatant was measured by ELISA. (F) HK-2 cells were treated with albumin (20 mg/ml) in the presence or absence of the caspase-1 inhibitor Z-VAD-fmk (5, 10, and 20 μ M). The levels of cleaved IL-18 and IL-1 β were measured by western blotting. The data are the means \pm SD from three separate experiments.

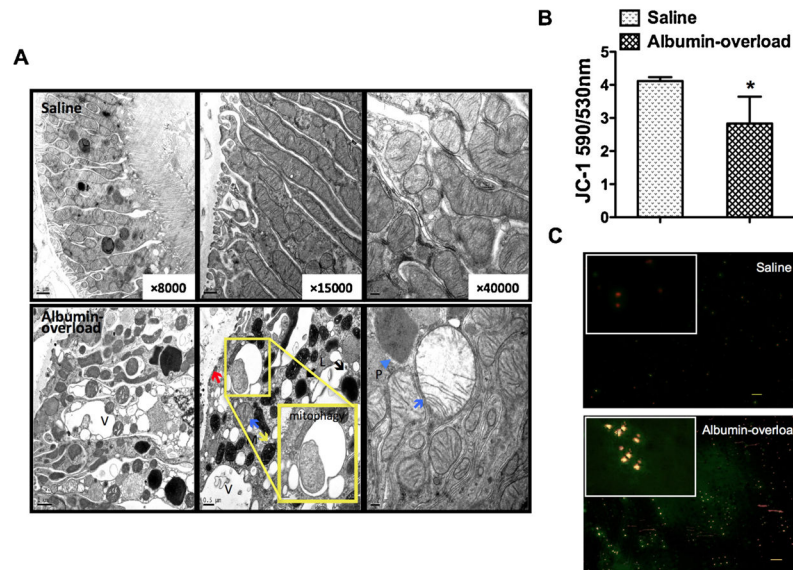


Fig. 5. Tubular cell stress and mitochondrial dysfunction. (A) The ultrastructure of tubular epithelial cells in saline-treated and albumin-overloaded Wistar rats was observed by TEM with different magnifications (8000 \times , 15,000 \times , and 40,000 \times). The upper images of the saline-treated group showed integrated tubular cells with normal and aligned mitochondria in the cytoplasm. The lower images depicted tubular basement membrane thickening (red arrow), and the tubular epithelial cells were flattened and destroyed with numerous vacuoles (V), peroxisomes (P, blue arrowhead), lysosomes (L), and visible mitophagy. The mitochondria (M) displayed “balloon-like” changes with oedema, disordered and absent cristae, and matrix brightness (blue arrow); however, mitochondrial pyknosis (yellow arrow) was also observed in the albumin-overloaded experimental rats. (B) JC-1 detection revealed that the extracted mitochondrial MMP from the tubular cells isolated from albumin-overloaded rats was markedly decreased compared with the saline-treated control group, as determined using a fluorescence microplate reader. The data are the means \pm SD ($n = 5$, $*P < 0.05$ vs. the saline-treated group). (C) JC-1 staining dyed the mitochondria isolated from the two groups, and these were observed by fluorescence microscopy. The red fluorescence reveals the normal MMP, whereas the green dye indicates reduced MMP. (For interpretation of the references to color in figure legend, the reader is referred to the web version of the article.)

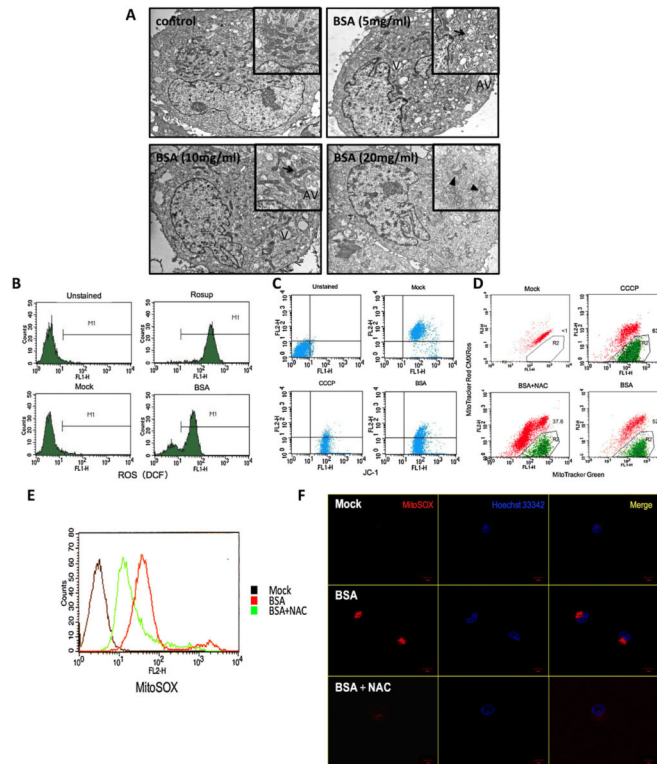


Fig. 6. The albumin-induced HK-2 cells experienced mitochondrial aberration and robust ROS production associated with Nlrp3 inflammasome activation. (A) TEM images of the morphological changes after BSA (5, 10, and 20 mg/ml) stimulation compared with medium alone. The HK-2 cells displayed a large amount of vacuoles (V) and autophagic vesicles (AV), and the results demonstrated that peroxisomes assembled in the cytoplasm after treatment with 5 mg/ml BSA. In the 10 mg/ml BSA group, the cells displayed slight mitochondrial oedema and phagosomes. Severe mitochondrial oedema and disappeared cristae were illustrated after exposure to a high level of BSA (20 mg/ml). (B) The total ROS generated by the HK-2 cells stimulated with BSA (20 mg/ml) for 24 h were analysed by flow cytometry by DCFH-DA staining. (C and D) HK-2 cells were stimulated with BSA (20 mg/ml) for 24 h or pre-incubated with NAC (50 mM) for 30 min before BSA exposure for 24 h, and CCCP (1 μ l), as a positive control of mitochondrial membrane depolarisation, was added for 30 min before staining. The cells were then stained with JC-1 (C), MitoTracker Red CMXRos and MitoTracker Green (D) and analysed by flow cytometry. (E and F) Flow cytometry (E) and confocal microscopy (F) analysis by MitoSOX staining of mitochondria-generated ROS in living HK-2 cells pre-treated or not pre-treated with 50 mM NAC and then treated with 20 mg/ml BSA.

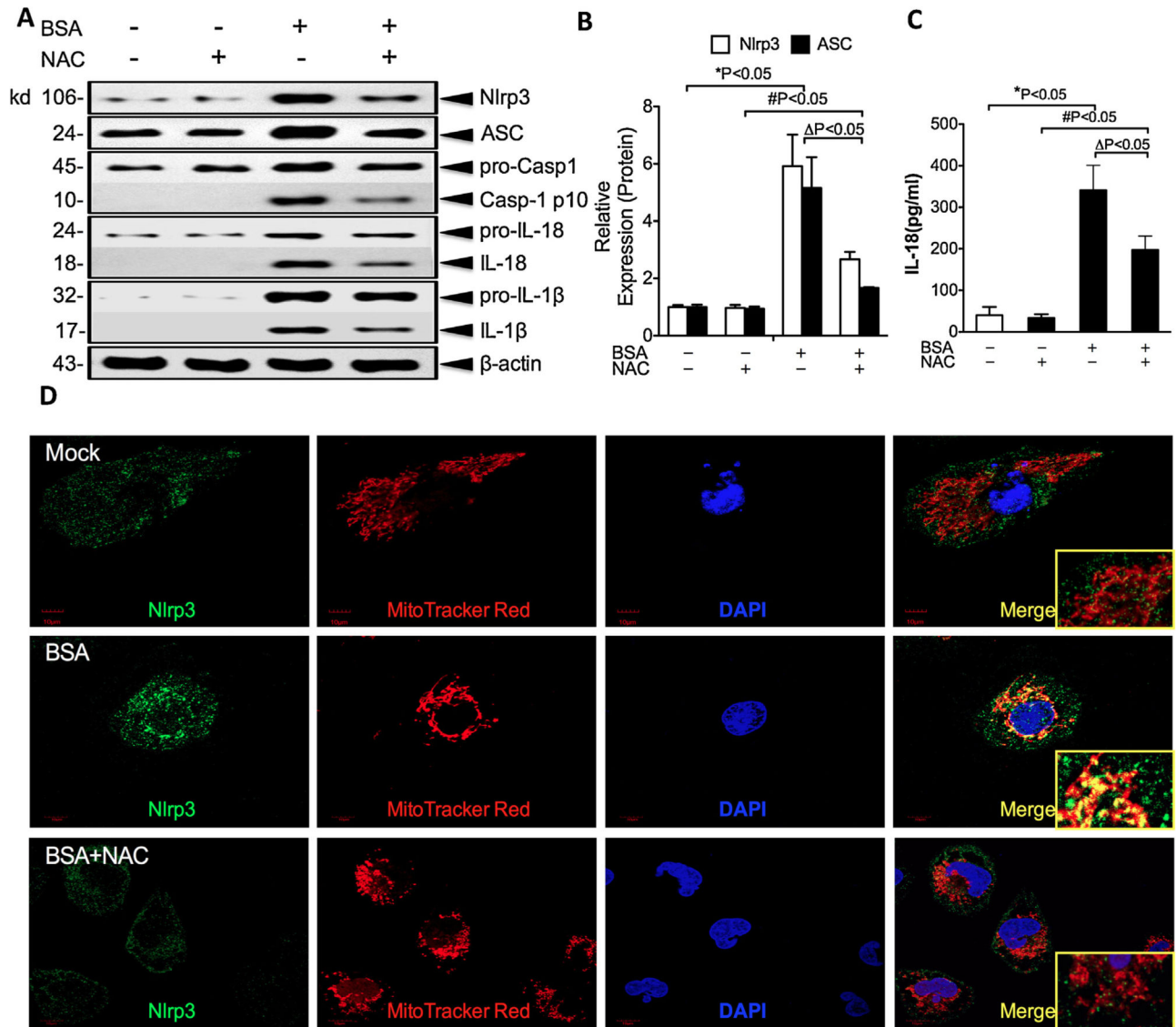


Fig. 7. Albumin-induced Nlrp3 inflammasome activation is prevented by a ROS scavenger in HK-2 cells. (A) The HK-2 cells were pre-incubated or not pre-incubated with NAC for 30 min and then treated with BSA (20 mg/ml) for 24 h. The levels of Nlrp3, ASC, pro-casp-1, pro-IL-18, and pro-IL-1 β expression in the cell lysates and caspase-1, IL-18, and IL-1 β expression in the supernatants were determined by western blotting. (B) Quantification of Nlrp3 and ASC protein expression in HK-2 cells normalised to that of β -actin. The data are presented as the means \pm SD from three independent experiments. * $P < 0.05$ vs. the control group, # $P < 0.05$ vs. the NAC control group. (C) The secreted IL-18 in the cell supernatants was measured by ELISA. (D) The expression of Nlrp3 in HK-2 cells and the co-localisation of Nlrp3 (green) with the mitochondria (Mitotracker Red) were analysed by confocal microscopy observation.

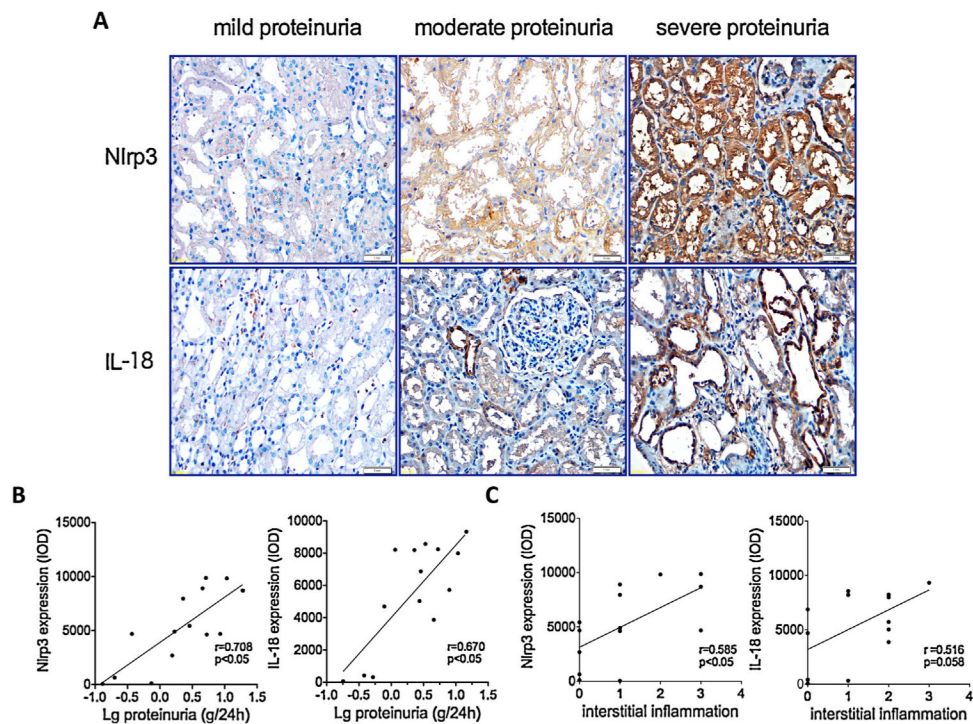


Fig. 8.

Nlrp3 inflammasome activation in renal biopsies of IgAN patients was associated with the degree of proteinuria. (A) Immunohistochemistry analysis of the Nlrp3 and IL-18 proteins localised in human renal biopsy specimens of IgAN patients. The sample was divided into three groups according to the degree of proteinuria: mild proteinuria (<math><1\text{ g/24 h}</math>), moderate proteinuria ($1\text{--}3.5\text{ g/24 h}$), and severe proteinuria (>3.5 g/24 h). (B) Correlation analyses summarised the correlations between the magnitude of proteinuria and the Nlrp3 or IL-18 protein level in renal biopsy samples. The data were compared using the Spearman correlation coefficient ($n = 16$). (C) Correlation analyses summarised the correlations between the tubulointerstitial inflammation and the Nlrp3 or IL-18 protein level in renal biopsy samples. The data were compared using the Spearman correlation coefficient ($n = 16$).

Tubular albumin overload

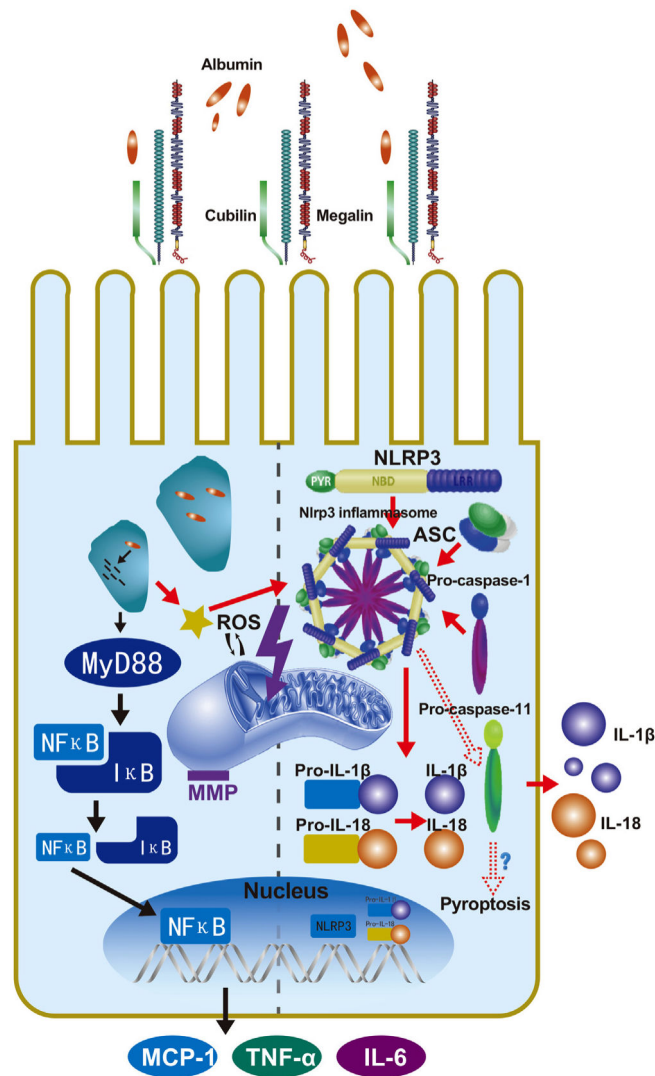


Fig. 9. The role of albumin overload in tubular epithelial cells. Under pathological conditions, albumin excessively filters over the capacity of reabsorption by proximal tubular cells. The albumin is endocytosed in the cytoplasm by megalin–cubilin receptors and induces MyD88–NF-κB signalling, which acts as a priming signal for Nlrp3, ASC and caspase-1 assembly. The priming process is associated with the NF-κB pathway, allowing Nlrp3 mRNA transcription and pro-cytokine preparation. Excessive albumin also leads to mitochondrial stress and ROS generation. Nlrp3 inflammasome activation by the detection of ROS release cleaves precursors of relative cytokines and secretes IL-1β and IL-18 to the interstitium for the subsequent inflammatory response.